

## Thymoquinone induces apoptosis in malignant T-cells via generation of ROS

Eileen Manasse Dergarabetian<sup>1</sup>, Khaled Imad Ghattass<sup>1</sup>, Sally Boulos El-Sitt<sup>1</sup>, Rasha Mahmoud Al Mismar<sup>1</sup>, Chirine Omar El-Baba<sup>4</sup>, Wafica Sami Itani<sup>1</sup>, Nada Mohamad Melhem<sup>2</sup>, Hiba Ahmad El-Hajj<sup>3</sup>, Ali Abdul Hamid Bazarbachi<sup>3</sup>, Regine Schneider-Stock<sup>4</sup>, Hala Uthman Gali-Muhtasib<sup>1</sup>

<sup>1</sup>Department of Biology, American University of Beirut, Beirut, Lebanon, <sup>2</sup>Medical Laboratory Sciences Program, American University of Beirut, Beirut, Lebanon, <sup>3</sup>Internal Medicine, American University of Beirut, Lebanon, <sup>4</sup>Experimental Tumor Pathology, Institute for Pathology, University Erlangen-Nuremberg, Germany

### TABLE OF CONTENTS

1. Abstract
2. Introduction
3. Methods
  - 3.1. Cell culture and treatments
  - 3.2. Viability assays
  - 3.3. Cell cycle analysis
  - 3.4. Hoechst staining
  - 3.5. Evaluation of mitochondrial transmembrane potential
  - 3.6. Cytochrome *c*
  - 3.7. Caspase activity
  - 3.8. Measurement of intracellular Glutathione levels
  - 3.9. Measurement of ROS
  - 3.10. Protein extraction and immunoblot analysis
  - 3.11. Annexin V staining
  - 3.12. Statistical analysis
4. Results
  - 4.1. TQ reduces viability and increases sub-G<sub>1</sub> population and apoptosis in malignant T cells, while PBMCs are more resistant
  - 4.2. TQ disrupts mitochondrial potential and releases cytochrome *c* in malignant T cells
  - 4.3. TQ induces caspase-dependent apoptosis
  - 4.4. TQ depletes GSH levels and increases ROS generation in malignant T cells
  - 4.5. Pretreatment with NAC and CAT protected malignant T cells against TQ-induced ROS generation and apoptosis
5. Discussion
6. Acknowledgements
7. References

### 1. ABSTRACT

We show that HTLV-1 negative leukemia cells are more sensitive to TQ due to higher levels of drug-induced reactive oxygen species (ROS). PreG<sub>1</sub> population in HTLV-1 negative Jurkat and CEM was higher than HTLV-1 transformed HuT-102 and MT-2 cells. Peripheral blood mononuclear cells were more resistant. Hoechst staining indicated more features of apoptosis, namely nuclear blebs and shrunken nuclei in HuT-102 than Jurkat. A greater depletion of the antioxidant enzyme glutathione occurred in Jurkat, which consequently led to an increase in ROS, loss of mitochondrial membrane potential, cytochrome *c* release, activation of caspases 3 and 9, and cleavage of PARP. Treatment with z-VAD-fmk partially reversed TQ-induced apoptosis, suggesting a caspase-dependent mechanism. N-acetyl cysteine prevented apoptosis providing evidence that cell death is ROS-dependent. Catalase prevented apoptosis to a lesser extent than NAC. In summary, TQ induces apoptosis in adult T cell leukemia/lymphoma by decreasing glutathione and increasing ROS, and levels of ROS underlie the differential cellular response to TQ. Our data suggest a potential therapeutic role for TQ in sensitizing HTLV-1-negative T-cell lymphomas.

### 2. INTRODUCTION

Regulation of cellular reactive oxygen species (ROS) is instrumental for maintaining redox homeostasis and any disruption in this regulation results in oxidative stress (1). The generation of ROS at a rate faster than their removal causes cell death through acute high levels of ROS or promotes carcinogenesis through chronic low levels of ROS (1). To maintain redox homeostasis, cells have ROS scavenging enzymes such as superoxide dismutase, glutathione peroxidase (GPX), glutathione reductase (GR), thioredoxin (TRX), and catalase. The O<sub>2</sub><sup>-</sup> free radicals generated by the mitochondrial electron transport chain and NADPH oxidase complex are reduced to the less reactive H<sub>2</sub>O<sub>2</sub> via endogenous supplies of superoxide dismutase (SOD). H<sub>2</sub>O<sub>2</sub> can in turn be reduced to H<sub>2</sub>O and O<sub>2</sub> by catalase (CAT) or in the presence of transition metals, such as Fe<sup>2+</sup> and Cu<sup>+</sup>, be converted to the extremely reactive, indiscriminate, and toxic HO (2). Glutathione (GSH) is the most abundant free thiol in eukaryotic cells which functions as a co-factor for GPX in which it provides two electrons for the reduction of H<sub>2</sub>O<sub>2</sub> to water. Thus, catalyzed by GPX, GSH in the presence of H<sub>2</sub>O<sub>2</sub> is converted to glutathione disulfide (GSSG) plus H<sub>2</sub>O (3,4). In this

manner, GPX functions in removing significant amounts of  $H_2O_2$ . Glutathione reductase (GR) is the antagonist of GPX, reducing GSSG back to GSH, thus ultimately replenishing anti-oxidant levels (4).

Cancer cells have increased levels of ROS that are known to promote cell proliferation, cell survival, and drug resistance (3). Targeting tumorigenic cells with redox altering strategies has recently gained interest as a possible approach for cancer therapy (5). Two different ROS-mediated therapeutic approaches have been proposed, one involves the use of anti-oxidants to abrogate ROS mediated signaling in cancer cells, and the other includes treating cancer cells with drugs that increase the generation of ROS and/or abrogate their antioxidant system. A pharmacological agent that generates ROS and inhibits ROS elimination functions as a double-edged sword. The therapeutic activity and selectivity of drugs is a major concern in anticancer drug discovery. Ideal drugs are those that are selectively toxic to malignant cells while not affecting normal cells and tissues. At present, there is only a limited number of selective drugs available for clinical use; therefore the development and design of novel compounds continues to be of interest to cancer researchers.

Thymoquinone (TQ) is the major bioactive component in black seed (*Nigella sativa*), an annual herb that grows in the Middle East, Western Asia, and Eastern Africa (6). There is growing interest in the therapeutic potential of TQ in different research fields, particularly in cancer therapy (7). TQ has been shown to decrease the proliferation of several neoplastic cells, including human breast and ovarian adenocarcinoma, myeloblastic leukaemia, HL-60, squamous carcinoma, SCC VII, fibrosarcoma, FSSaR, laryngeal neoplastic cells-Hep-2, and prostate and pancreatic cell lines (reviewed in 6). Although the exact mechanisms of TQ action are not fully elucidated, recent reports have shown that TQ induces apoptosis by the generation of ROS. This has been documented in primary effusion lymphoma (8), HL-60 leukemia (9), colon cancer cells (10), prostate cancer cells (11), and lymphoblastic leukemia cell line (12). Interestingly, several normal cells were found to be resistant to TQ. These include human pancreatic ductal epithelial cells, prostate epithelial (BPH-1) cells, and normal human intestinal (FHs74Int) cells (10,13,14).

Adult T cell leukemia/lymphoma (ATL) is a malignancy of mature activated  $CD4^+$  T cells associated with the human T-cell lymphotropic virus type I (HTLV-I infection). HTLV-I transactivator protein Tax activates several major cellular transcription factor pathways which mediate viral transformation (reviewed in 15). The median survival of ATL patients is less than one year mainly because of resistance to conventional and high dose chemotherapy (16). Since TQ effects on ATL are not known, here, we investigated the antitumor activity of TQ against four adult T cell leukemia/lymphoma cell lines, two of which are HTLV-I negative (CEM and Jurkat) and two are constitutively expressing the virus (MT-2 and HuT-102). Our data provide evidence that TQ induces apoptosis

in malignant T cells via a mechanism involving the depletion of GSH and subsequent generation of ROS. HTLV-I negative cells were more sensitive to TQ-induced apoptosis. Cell death by TQ was associated with mitochondrial membrane disruption, cytochrome c release, and caspase activation. Considering the higher resistance of HTLV-positive cells to TQ-induced apoptosis, the present study suggests a potential therapeutic role for this promising molecule in sensitizing HTLV-I-negative T-cell lymphomas.

### 3. METHODS

#### 3.1. Cell culture and treatment

HTLV-I positive (HuT-102 and MT-2) and HTLV-I negative (CEM and Jurkat)  $CD4^+$  malignant T-cell lines were cultured in RPMI 1640 medium (Invitrogen Molecular Probes, Eugene, OR, USA) containing 10% heat inactivated fetal bovine serum (FBS) and 1% penicillin-streptomycin (Invitrogen Molecular Probes, Eugene, OR, USA) in a humidified incubator (95% air, 5%  $CO_2$ ). Peripheral blood mononuclear cells (PBMC) were isolated, after obtaining informed consent approved by the Institutional Review Board, from blood of four healthy HTLV-I-negative donors, using Ficoll-Hypaque (Lymphoprep, Nyegaard, Norway). Activated PBMC were grown in Ham's F10 medium (Sigma, St. Louis, MO, USA) supplemented with IL-2 (1microg/10ml) (Roche, Mannheim, Germany). Unless otherwise mentioned, cells were seeded ( $2 \times 10^5$  cells/ml) and treated at 50% confluency with TQ (MP Biomedicals, France) dissolved in methanol. The final methanol concentration did not exceed 0.1%. For determining ROS involvement, cells were pre-treated with 5 mM N-acetyl cysteine (NAC) (Sigma, St. Louis, MO, USA), 500 U/ml catalase (Sigma, St. Louis, MO, USA), or 100 microM buthionine sulfoximine (BSO) (Sigma, St. Louis, MO, USA) prior to TQ. CAT was dissolved in 50 mM potassium phosphate buffer, pH 7.0. To examine caspase involvement in TQ-induced apoptosis, the general caspase inhibitor (zVAD-fmk) (Calbiochem, Darmstadt, Germany) was added at 30 microM for 2 hours before TQ.

#### 3.2. Viability assays

Cells were seeded ( $1 \times 10^5$  cells/ml) in 96-well plates and treated the next day with vehicle (0.1% methanol) or with TQ (1, 5, 10, 40 or 100 microM). Cell viability was assessed by the CellTiter 96® non-radioactive cell proliferation assay kit according to the manufacturer's instructions (Promega Corp, Madison, WI, USA). In this assay the ability of metabolically active cells to convert 3-(4,5-dimethyl thiazol-2-yl)-2,5-diphenyl tetrazolium bromide (MTT) into a blue formazan product is measured and its absorbance is recorded at 595 nm using an enzyme-linked immuno-sorbent assay (ELISA) microplate reader. Results are expressed as % viability relative to control. Cell viability was also confirmed by trypan blue dye exclusion (data not shown).

#### 3.3. Cell cycle analysis

Cells were seeded in 6-well plates, treated with TQ, washed twice with cold PBS, fixed in ice cold 70%

ethanol, and stored for 24 hours at  $-20^{\circ}\text{C}$ . Subsequently, they were rinsed with PBS, incubated for 30 min at  $37^{\circ}\text{C}$  with PBS, 1 % RNase A (Roche, Mannheim, Germany), and PI (100 microg/ml final concentration) (Invitrogen Molecular Probes, Eugene, OR, USA). Supernatants were then transferred to flow tubes and read at the FL-2 channel. Cell cycle analysis was performed using FACS scan flow cytometer (Becton Dickinson, Franklin Lakes, NJ, USA). 10,000 events were collected per sample and the analysis of corresponding cell cycle distribution was performed using CellQuest software (Becton-Dickinson, Franklin Lakes, NJ, USA).

### 3.4. Hoechst staining

Cells were seeded in 6-well plates, treated and spun down at 500 g for 5 min, then washed with 1x PBS. This was followed by fixing in 75% ice-cold ethanol and overnight incubation at  $-20^{\circ}\text{C}$ . Cells were then washed with 1x PBS and re-suspended in PBS and cytospun with single cytology funnels (Fisherbrand, Houston, TX, USA). Approximately 180,000 cells/condition were cytospun at 1500 rpm for 5 min. Once cells attached to slides, Hoechst stain (0.5microl stock solution in 10ml 1x PBS) (Invitrogen Molecular Probes, Eugene, OR, USA) was added for 5 min in the dark. Cells were then washed twice with PBS in the dark and a drop of fluorosave (Calbiochem, Darmstadt, Germany) was added. Slides were kept at  $-20^{\circ}\text{C}$  overnight, after which images were captured using a confocal microscope at 60X magnification. The Hoechst stain is excited by UV light at 305nm and emits blue fluorescing light at an emission of 461 nm.

### 3.5. Evaluation of mitochondrial transmembrane potential

Rhodamine-123 (Sigma, St. Louis, MO, USA) was used to monitor the integrity of mitochondria following drug treatment as described previously (17). Cells were cultured in 60-mm<sup>2</sup> dishes ( $10^5$  cells/ml), treated with TQ for 48 hours, and then harvested by centrifugation. After washing with rhodamine buffer, pelleted cells were resuspended in 500 microl buffer containing 5 microM of rhodamine dye 123 (Sigma, St. Louis, MO, USA) and incubated for 30 min at  $37^{\circ}\text{C}$ . Fluorescence emission at 525nm after excitation at 488nm was quantified by FACScan flow cytometry using the CellQuest software.

### 3.6. Cytochrome c

A cytochrome c enzyme-linked immunosorbent assay (ELISA) kit (Invitrogen Molecular Probes, Eugene, OR, USA) was used to determine if TQ treatment resulted in the translocation of cytochrome c from the mitochondria to the cytosol. The assay was performed according to the manufacturer's instructions. Briefly, cells were plated in six-well plates and allowed to adhere for 24 hours, after which the cells were treated with increasing concentrations of TQ for an additional 24 hours for Jurkat cells and 48 hours for HuT-102 cells. The cells were spun and the supernatant collected as the cytosolic fraction. Optical density of each well was determined using a microplate reader set to 450 nm. Results are expressed as picograms of cytochrome c per milligram of protein.

### 3.7. Caspase activity

Activity of caspases 3 and 9, which have an important role in the intrinsic apoptotic pathway, was measured using the caspase sampler kit (Biosource, Camarillo, CA). Each sample contained  $3-5 \times 10^6$  cells and was assayed in duplicates according to manufacturer's instructions.

### 3.8. Measurement of intracellular Glutathione levels

GSH levels were determined after 2 hours of TQ treatment with or without pre-treatment with the glutathione inhibitor BSO (100 microM, 24 hours). Free Glutathione levels were measured using the Glutathione Colorimetric Detection Kit (Arbor Assays, MI, USA) according to the manufacturer's instructions. Briefly,  $5 \times 10^6$  cells/condition were cultured in T75 flasks, then treated and washed with 1x PBS at 600g for 5 min, after which 1% 5-sulfosalicylic acid dehydrate (SSA) (Sigma, St. Louis, MO, USA) was added. The pellets were lysed by vortexing in 5% SSA and incubated on ice for 10 min. Samples were then centrifuged at 1400 rpm for 10 min and 4 ml of Assay Buffer was added to the supernatant. 50microl of the supernatant containing acid-soluble thiols was added to single wells of a 96-well microtiter plate and treated with 2-vinylpyridine (2VP) (Sigma, St. Louis, MO, USA), which allows the quantification of oxidized glutathione (GSSG). Following 2VP treatment, 50 microl supernatant was transferred into 96-well plate. Optical density (OD) was measured at 405 nm using an ELISA microplate reader. The concentrations of GSH and GSSG were calculated from a titration curve established using known concentrations of purified GSH and GSSG.

### 3.9. Measurement of ROS

Generation of intracellular  $\text{H}_2\text{O}_2$  was measured using 5-(and-6)-chloromethyl-2',7'-dichlorodihydrofluorescein diacetate, acetyl ester (CM-H2DCFDA) kit (Invitrogen Molecular Probes, Eugene, OR, USA), a derivative of the DCFDA but with an additional thiol reactive chloromethyl group that enhances the ability of the compound to bind to intracellular components. CM-H2DCFDA is non-fluorescent until removal of the acetate groups by intracellular esterases and oxidation by  $\text{H}_2\text{O}_2$  to form the highly fluorescent derivative 2'-7'-dichlorofluorescein (DCF). Cells were cultured in 6-well plates, spun down, washed with 1x PBS, and pellets were re-suspended in 500 microl RPMI containing 2% FBS and 10 microM CM-H2DCFDA for 20 min at  $37^{\circ}\text{C}$  in the dark in 1.5 ml eppendorf tubes. Subsequently, cells were pre-treated with  $\text{H}_2\text{O}_2$  (150 microM) for 40 min, with NAC (5mM) for 2 hours, or CAT (500 U/ml) for 5 min followed by 1 hour TQ treatment, then washed once with 1x PBS and analyzed with FACS scan flow cytometer on the FL-1 channel with excitation set at 488 nm and emission at 530 nm.

### 3.10. Protein extraction and immunoblot analysis

For total cellular protein extraction, the buffer contained 50 mM Tris-HCl, pH 7.5, 150 mM NaCl, 1% Nonidet P40, 0.5% sodium deoxycholate, 4% protease inhibitors and 1% phosphatase inhibitors. Protein concentration was determined using DC BioRad protein

assay kit (BioRad Laboratories, Hercules, CA, USA) with bovine serum albumin as standard. Cellular proteins were then loaded onto SDS-polyacrylamide gel and the supernatant protein bands were then transferred by blotting using nitrocellulose membranes. The blots were blocked at room temperature in 5% skimmed milk in TBS (50mM Tris-HCl and 150mM NaCl) and probed overnight with primary antibody at 4°C. The primary antibodies used were all from Cell Signaling (Beverly, MA, USA) (caspase 3, #9662s; caspase 9, #9502; PARP, #9532s; Bax, #5023s; Bcl-2, #2870s). In order to ensure equal protein loading the GAPDH antibody was used. The detection of the protein bands was done with enhanced chemiluminescence system (ECL).

### 3.11. Annexin V staining

Apoptosis was determined by Annexin V staining according to manufacturer's instructions (Roche, Mannheim, Germany). Briefly, cells were seeded in 6-well plates, treated with TQ, and then centrifuged at 1500 rpm for 10 min, 4°C and washed with 1X PBS. The pellet was resuspended in 100 microl Annexin-V-Fluos labeling solution (20 microl annexin reagent and 20 microl PI (50 microg/ml) (in 1000 microl incubation buffer pH 7.4 (10 mM Hepes/NaOH, 140 mM NaCl, 5 mM CaCl<sub>2</sub>)). The samples were incubated for 15 min at room temperature and 0.45 ml incubation buffer was added. The cellular fluorescence was then measured by flow cytometry using a Fluorescence Activated Cell Sorter (FACS) flow cytometer. 10,000 events were collected and the analysis of corresponding cell cycle distribution was determined using CellQuest software.

### 3.12. Statistical analysis

Statistical analysis was performed on raw data using SPSS v16.0. One way analysis of variance (ANOVA) followed by Tukey's test was used to compare multiple treated samples versus a single control while a one tailed t-test was used to compare any significant difference between any two samples. Statistical significance was assumed when the *p*-value was less than 0.05.

## 4. RESULTS

### 4.1. TQ reduces viability and increases sub-G<sub>1</sub> population and apoptosis in malignant T cells, while PBMC are more resistant

HTLV-1 transformed (MT-2 and HuT-102) and HTLV-1 negative (CEM and Jurkat) malignant T-cell lines were treated with different concentrations of TQ (1-100microM) for 24, 48, or 72 hours to determine possible dose- and time- dependent inhibitory effects on cell viability. As shown in Figure 1, 100 microM TQ for 72 hours inhibited cell viability by 100% in all T-malignant cell lines. The HTLV-1 negative cell lines were more sensitive to TQ than the HTLV-transformed cells (Figure 1). IC<sub>50</sub> values at 48 hours were 8 microM in CEM, 28 microM in Jurkat, 35 microM in MT-2 and 85 microM in HuT-102. Interestingly, normal Peripheral Blood Mononuclear Cells (PBMC) were more resistant to TQ (Figure 1). Treatment with 40 or 100microM TQ for 48 hours reduced the viability of PBMC by only 27% in comparison to 60% and 50% reduction in Jurkat and HuT-102 cells, respectively.

To determine the mode of cell death induced by TQ, we exposed HTLV-1 negative and positive cell lines to 10, 40 or 100 microM TQ for 48 hours and analyzed cells by PI staining of DNA with flow cytometry (Figure 2) and by Hoechst staining (Figure 3A). The results revealed that TQ caused an accumulation of cells in the sub-G<sub>1</sub> phase in all four cell lines, effects that were more pronounced in the HTLV-1 negative cell lines (Figure 2). At 40 microM TQ after 48 hours, 80% of CEM cells and 75% of Jurkat cells accumulated in the sub-G<sub>1</sub> phase in comparison to only 26% in MT-2 and 11% in HuT-102. In CEM and Jurkat cells, the increase in sub-G<sub>1</sub> by TQ was accompanied with a significant decrease in the G<sub>0</sub>/G<sub>1</sub>, S and G<sub>2</sub>/M populations; however, in HuT-102 and MT-2 cells, TQ treatment only reduced the G<sub>0</sub>/G<sub>1</sub> population but did not affect the percentage of cells in the S and G<sub>2</sub>/M phases (Figure 2). Fluorescent microscopy images of Hoechst stained cells indicated features of apoptosis such as nuclear blebs and shrunken nuclei in TQ-treated malignant T cells (Figure 3A). The higher sensitivity of HTLV-1 negative Jurkat cells was also confirmed by the Hoechst assay.

### 4.2. TQ disrupts mitochondrial potential and releases cytochrome c in malignant T cells

During apoptosis, the process of mitochondrial membrane disruption represents a point of no return as it commits the cell to death. To investigate if TQ causes loss of mitochondrial membrane potential, cells were treated with 10, 40 or 100 microM TQ for 48 hours and mitochondrial membrane potential ( $\Delta\psi_m$ ) was assessed by the rhodamine assay with flow cytometry. As shown in Figure 3B, TQ induced a significant dose-dependent decrease in mitochondrial transmembrane potential, particularly in Jurkat cells. The percentages of Jurkat cells with reduced rhodamine123 fluorescence after 10 and 40 microM TQ was 65% and 83%, respectively, in comparison to only 4% and 31% in HuT-102. We further examined whether this disruption in mitochondrial membrane correlates with an increase in cytochrome c release. Treatment of Jurkat (24 hours) and HuT-102 (48 hours) cells with 10, 40 or 100 microM TQ significantly increased the release of cytochrome c into the cytosol as revealed by ELISA (Figure 3C). In Jurkat cells, TQ increased the levels of cytosolic cytochrome c by 8-10 fold in comparison to only 2-4 fold increase in HuT-102.

The role of mitochondria in TQ-induced apoptosis was further studied by examining the effects of a 24 hour treatment with TQ (10, 30 and 50 microM) on the levels of the Bcl-2 family members: Bax and Bcl-2 (Figure 4A), which are important players in the intrinsic apoptotic pathway. Western blot revealed a significant decrease in Bcl-2 protein and an increase in Bax in Jurkat cells treated with 30 and 50 microM TQ, further confirming the direct role of mitochondria in TQ-induced apoptosis. Conversely, the levels of both proteins were not changed in HuT-102 cells in response to TQ.

### 4.3. TQ induces caspase-dependent apoptosis

Caspase activation is one mechanism through which many anticancer drugs induce apoptosis. We and others have shown that TQ-mediated apoptosis in leukemia, colon cancer and osteosarcoma cell lines is caspase

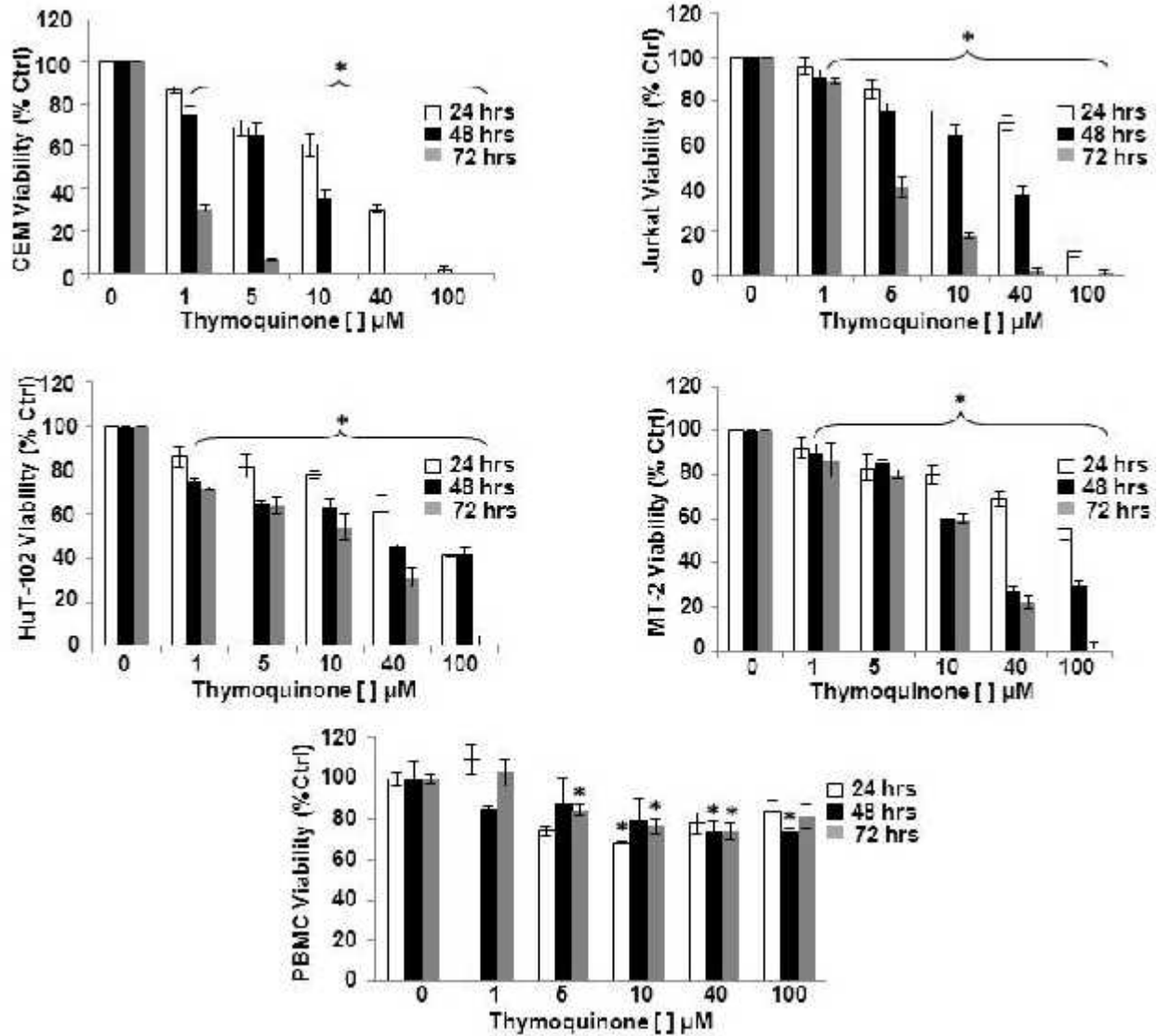


**Figure 1.** TQ reduces the viability of malignant T cells while peripheral blood mononuclear cells (PBMC) are more resistant. HTLV-1 negative (CEM and Jurkat) and HTLV-1 positive (MT-2 and HuT-102) malignant T-cell lines and PBMC were treated with TQ for up to 72 hours. PBMC were obtained from four healthy donors. Cell viability (expressed as percentage of control) was determined using the Cell Titer 96 non-radioactive cell proliferation kit as described in "Materials and Methods". Each value is the mean  $\pm$  SD of four separate experiments each done in triplicates. \*significantly different ( $p < 0.05$ ) from control for each time point using one-way ANOVA followed by Tukey's test.

dependent (18,19,20), while apoptosis by TQ in prostate cancer cells has been shown to be independent of caspases (11). To investigate whether TQ causes activation of caspases in malignant T-cells, we assayed for caspases 3 and 9 by western blot analysis (Figure 4A) and by ELISA (Figure 4B) in Jurkat and HuT-102 cells treated with 10, 30 or 50 microM TQ for 24 hours. The antibodies used recognize both the procaspases and the cleaved activated forms of these enzymes. TQ treatment resulted in the cleavage of caspase 3 to its 17 kDa active form and enhanced caspase 3 activity by 7 fold at 50 microM in Jurkat (Figures 4A,B). TQ also induced the activation and cleavage of caspase 9 in Jurkat more than HuT-102 cells.

The nuclear enzyme PARP is a 116 kDa that is a caspase substrate, and cleavage of PARP from the 116 kDa to 85 kDa form can be detected in caspase-dependent apoptosis. As shown in Figure 4A, TQ induced the cleavage of PARP in both cell lines.

To investigate whether caspases participate in TQ-induced apoptosis, we pre-treated Jurkat and HuT-102 with the general caspase inhibitor z-VAD-fmk (30 microM for 2 hours) followed by TQ and performed FITC-Annexin V/PI staining after 48 hours. During apoptosis, the asymmetry in the phospholipid membrane is disrupted, leading to the exposure of phosphatidylserine on the outer

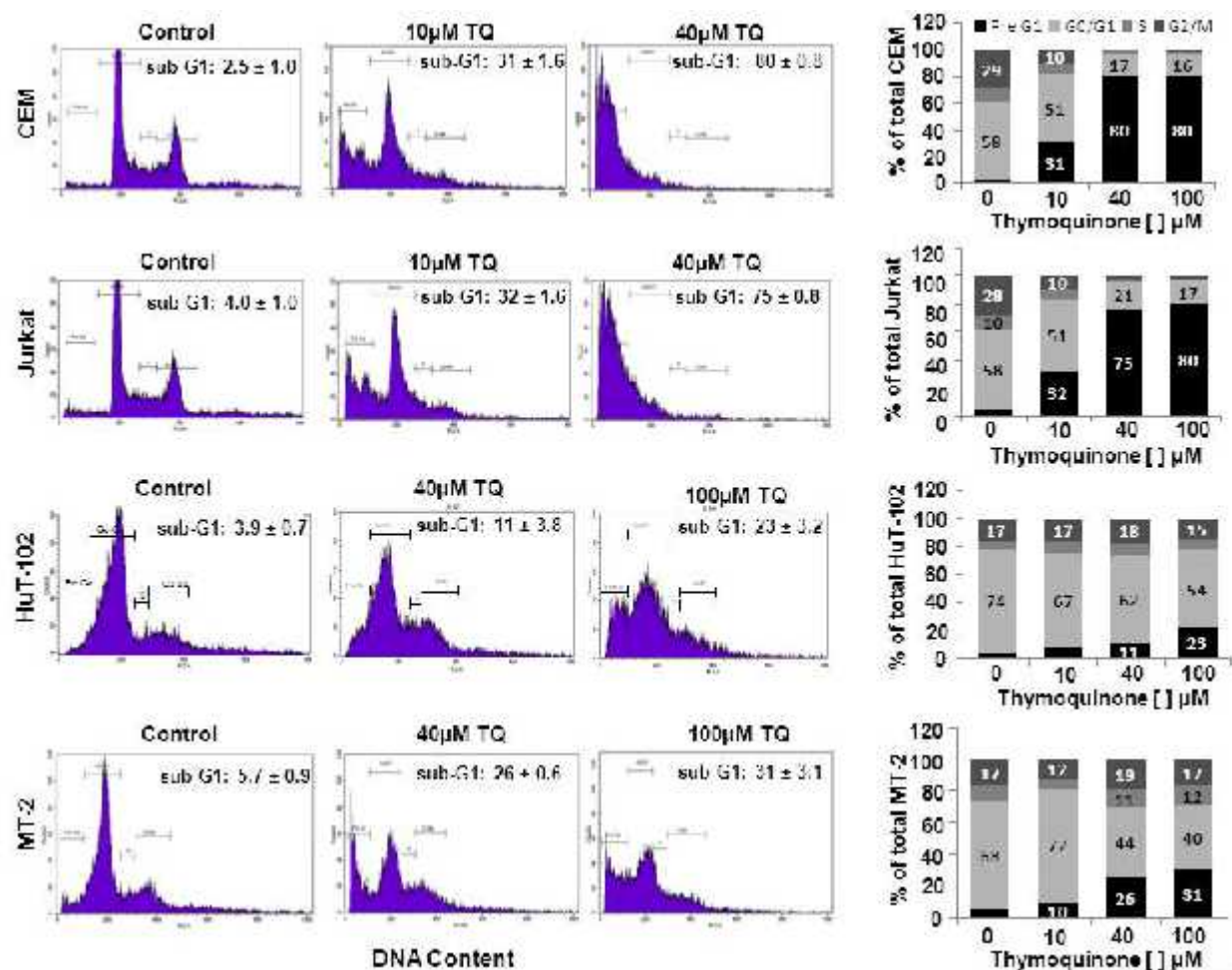


**Figure 2.** TQ increases the sub-G1 population in CEM and Jurkat more significantly than MT-2 and HuT-102 cells. Cells were treated with 10, 40 or 100 microM of TQ for 48 hours after which they were stained with PI for flow cytometric analysis of DNA content with FACScan flow cytometry as described in “Materials and Methods”. The percentage of cells in the various stages of the cell cycle was calculated using Cell Quest. Each value is the mean of two separate experiments each done in duplicates.

leaflet of the plasma membrane which binds to Annexin V. The results presented in Figure 4B show that in the presence of z-VAD-fmk, Annexin positive cells (early and late apoptotic) decreased from 60% to 20% in Jurkat and 18% to 10% in HuT-102, respectively, in the presence of z-VAD-fmk, suggesting that apoptosis by TQ is caspase-dependent.

#### 4.4. TQ depletes GSH levels and increases ROS generation in malignant T cells

It has been recently shown that, in prostate cancer cells, TQ inhibits levels of Glutathione (GSH), the most abundant non-protein thiol in mammalian cells known to play a key role in protecting cells against oxidation (11). Therefore, we investigated the role of TQ in depleting intracellular levels of GSH in malignant T cells (Figure 5A). Jurkat and HuT-102 cells were treated with TQ (5-100 microM) and the levels of GSH were measured colorimetrically 2 hours later (Figure 5A). Treatment with TQ clearly resulted in a dose-dependent decrease in GSH levels in both Jurkat and HuT-102 cells, and the decrease

was more pronounced in Jurkat cells. Interestingly the extent of GSH depletion in Jurkat cells by 40 microM TQ was similar to pre-treatment with the strong GSH inhibitor BSO (Figure 5A). It is known that GSH depletion results in high levels of ROS that are involved as intermediates in the signal transduction pathways of apoptosis (21). Moreover, it has been shown by our group and by others that TQ induces apoptosis *via* the generation of ROS (8,10,11). Therefore, we determined the effect of TQ on ROS production in malignant T cells and normal PBMC. Cells were treated with 10 or 40 microM TQ for 1 hour and ROS levels were measured using the CM-H2DCFDA molecule (Figure 5B). In both HuT-102 and Jurkat cells, treatment with 40 microM TQ elicited a significant increase in ROS production comparable to the addition of 150 microM H<sub>2</sub>O<sub>2</sub> (Figure 5B). A dose-dependent increase in ROS generation was clearly evident in both cell lines and the oxidant shift was greater in Jurkat than HuT-102 (64% in Jurkat vs. 25% in HuT-102). In contrast, treatment of the resistant normal PBMC with 10 or 40 microM TQ did not cause any increase in ROS levels (Figure 5B). These results suggest

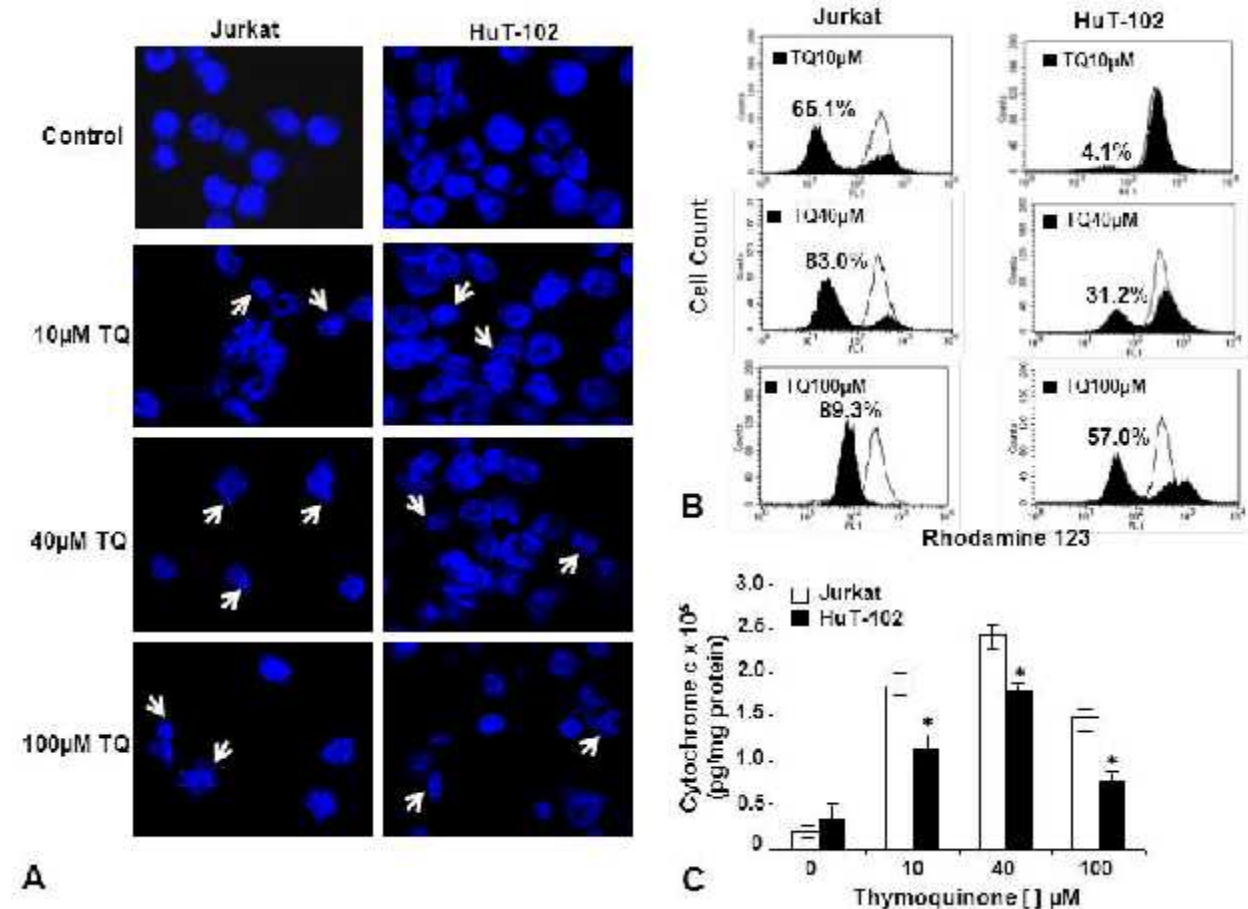


**Figure 3.** TQ causes more DNA fragmentation and mitochondrial membrane disruption in Jurkat than HuT-102 malignant T cells. (A) Fluorescent microscopy images of Hoechst stained Jurkat and HuT-102 cells at 48 hours after treatment with 10, 40 or 100 microM TQ. White arrows indicate features of apoptosis such as nuclear blebs and shrunken nuclei. (B) Cells were treated with TQ for 48 hours and loss of mitochondrial membrane potential was determined by rhodamine-123 retention as described in “Materials and Methods”. Panels represent overlay of rhodamine-123 fluorescence of TQ-treated cells (solid graphs) over control cells (open graphs) with the corresponding percentage of rhodamine leakage in 10,000 gated cells. Results are representative of two independent experiments. (C) Cytochrome c was measured by ELISA in Jurkat (24 hours) and HuT-102 (48 hours) in response to treatment with TQ, and the results shown are mean optical density values  $\pm$  SD of two independent experiments each in duplicate. \*significantly different ( $p < 0.05$ ) from Jurkat at each TQ concentration using one-way ANOVA followed by Tukey’s test.

that the depletion of GSH levels and increase in ROS generation appear to play a role in TQ-induced inhibition in cell viability and apoptosis in malignant T cells.

#### 4.5. Pretreatment with NAC and CAT protected malignant T cells against TQ-induced ROS generation and apoptosis

To confirm the role of ROS in TQ-mediated inhibition in cell viability and apoptosis, ROS levels were monitored in Jurkat and HuT-102 cells pretreated with NAC (5mM for 2 hours) or CAT (500U/ml for 5 min) followed by 40 microM TQ and CM-H<sub>2</sub>DCFDA staining (Figure 6A). NAC is a widely used thiol containing antioxidant that scavenges ROS and functions as a precursor of GSH, while CAT breaks down H<sub>2</sub>O<sub>2</sub> into H<sub>2</sub>O and O<sub>2</sub>. We observed that NAC and CAT pretreatment significantly inhibited TQ-induced ROS generation in both

Jurkat and HuT-102 cells. The increase in ROS generation by TQ was inhibited more by pretreatment with NAC than by CAT (Figure 6A).

In order to study the effects of NAC and CAT on TQ-induced inhibition in cell viability and apoptosis, cells were pretreated with 5 mM NAC for 2 hours or 500U/ml CAT for 5 min and then exposed to 40 microM TQ and 48 hours later cell viability was measured by trypan blue (Figure 6B), while apoptosis was determined by Annexin staining (Figure 6C). The NAC and CAT control groups did not show any inhibition in cell viability or apoptosis compared with untreated controls. Pretreatment with NAC significantly protected both Jurkat and HuT-102 cells against the growth inhibitory and apoptotic effects of TQ (Figure 6B, C). In Jurkat cells, the viability increased from 12 % (-NAC) to 80% (+NAC) at 40 microM TQ, while

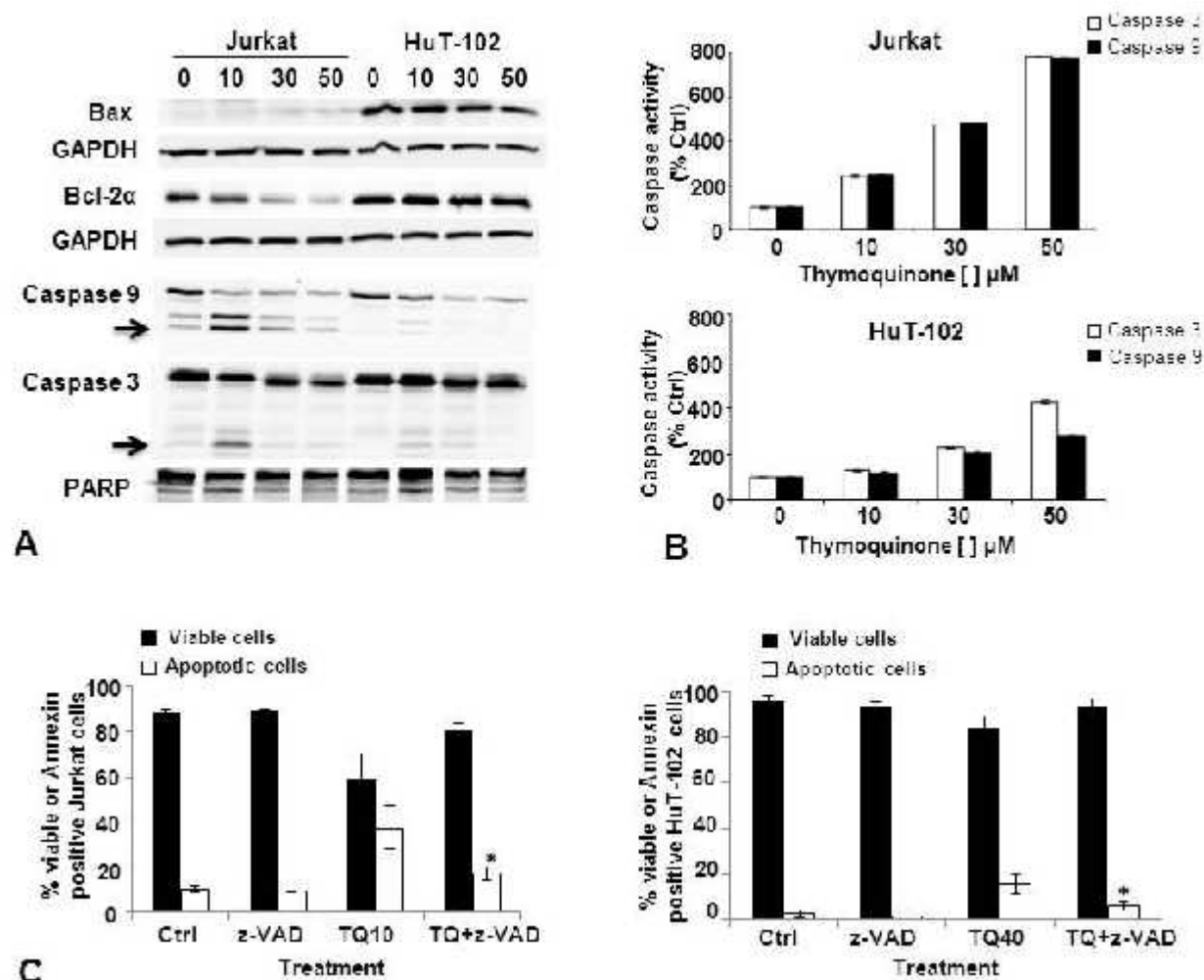


**Figure 4.** TQ-induced apoptosis is caspase-dependent. (A) Cells were treated with TQ for 24 hours and whole cell lysates were immunoblotted with Bax, Bcl-2, caspase 3, caspase 9 and PARP. All blots were re-probed with GAPDH to ensure equal protein loading. (B) Activity of caspases 3 and 9 was measured in duplicates in samples containing  $3-5 \times 10^6$  cells using the caspase sampler kit. Results are expressed as % of control cells from two independent experiments. (C) Cells were pre-treated with 30 microM of the caspase inhibitor zVAD-fmk for 2 hours followed by 10 microM TQ (Jurkat) or 40 microM TQ (HuT-102) for 48 hours, after which cells were stained with fluorescein-conjugated annexin V and PI. Apoptotic cells were analyzed by flow cytometry. The graphs display the means  $\pm$  SD of two separate experiments each in duplicate. \*significantly different ( $p < 0.05$ ) from TQ alone using one-way ANOVA followed by Tukey's test.

HuT-102 displayed a less significant increase in viability from 60% (-NAC) to 78% (+NAC) (Figure 6B). In accordance with the ROS data, NAC pretreatment significantly protected malignant T cells against TQ-induced apoptosis more than CAT, which may be due to the fact that NAC acts not only as a ROS scavenger but also replenishes the intracellular GSH enzyme that is depleted by TQ. Taken together, these results suggest that the depletion of GSH and increased ROS generation are responsible for TQ-mediated cell death.

## 5. DISCUSSION

Adult T cell leukemia is an aggressive malignancy caused by HTLV-1 which remains of poor

prognosis despite recent progress in ATL therapy because of intrinsic chemoresistance and severe immunosuppression (15). The viral Tax oncoprotein plays an important role in initiating the disease and in activating major cellular transcription factor pathways leading to resistance to therapy (reviewed in 15). Therefore, the search for new effective drugs is warranted to reduce chemotherapy resistance and the poor treatment outcome encountered in ATL patients.

Although several studies have shown that the plant-derived compound Thymoquinone (TQ) possesses anti-neoplastic activities in several tumor models, the effect of TQ on HTLV-1 negative and positive leukemia cell lines has not been determined before. Here, we show that

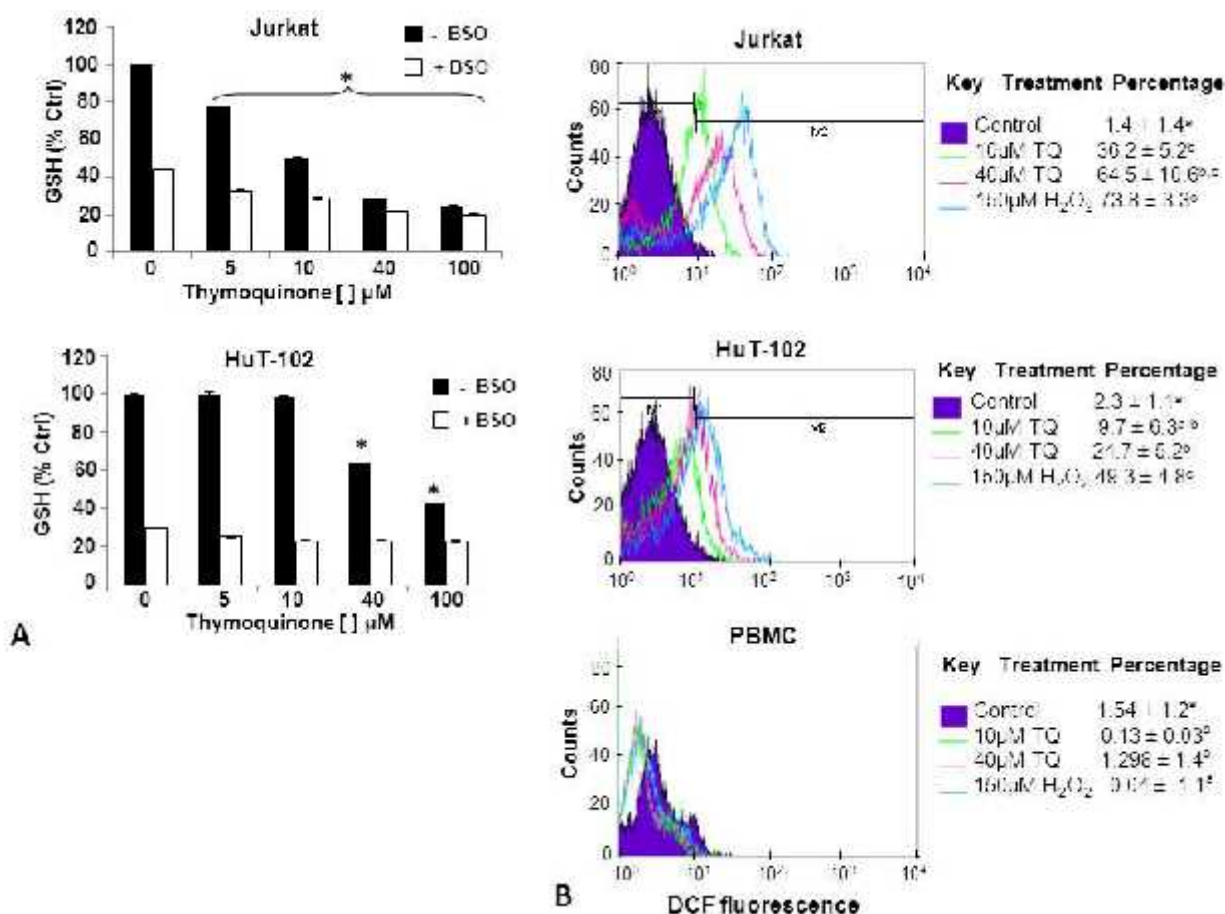


**Figure 5.** TQ causes depletion of intracellular GSH levels and increase in ROS generation more significantly in Jurkat than HuT-102 cells, while PBMC are resistant to TQ-induced oxidative stress. (A) Cells were pre-treated or not with 100 microM BSO for 3 hours, followed by TQ treatment for 2 hours. Immediately after TQ, colorimetric detection of GSH was done in a 96-well plate reader at 405 nm as described in “Materials and Methods”. Each value is the mean  $\pm$  SD of two separate experiments. \*significant difference ( $p < 0.05$ ) by one-tailed t-test between TQ treated and untreated samples. (B) Cells were treated with 10 microM CM-H2DCFDA dye for 20 mins, and then with TQ or H<sub>2</sub>O<sub>2</sub> for 1 hour. Immediately after, cells were harvested and the amount of DCF fluorescence was analyzed by flow cytometry.

HTLV-1 negative leukemia cells are more sensitive to TQ due to the higher levels of ROS produced in these cells in response to TQ treatment. TQ induced a concentration and time-dependent cytotoxicity in a panel of adult T cell leukemia/lymphoma cell lines while normal PBMC were resistant. The IC<sub>50</sub> values of 28 microM (Jurkat) and 85 microM (HuT-102) after 48 hours of TQ treatment indicate that TQ is about 3 times more toxic to HTLV-1 negative Jurkat than the HTLV-1 positive HuT-102 cells. TQ toxicity in malignant T-lymphocytes is attributed to apoptosis as evidenced by caspase 3 and 9 activation, flow cytometry analysis showing an increase in sub-G1 DNA content, and the characteristic morphological features observed in Hoechst stained DNA. A significant number of cells show apoptotic crescent-shaped nuclei, and nuclear blebs thereby confirming an apoptotic mode of cell death. Treatment with the general caspase inhibitor z-VAD confirmed caspase-dependent apoptosis. These results are in accordance with previous work from our lab and others which point to TQ's pro-apoptotic ability in several cancer

cell lines including human colon cancer (22), osteosarcoma (19), neoplastic keratinocytes (23), human breast cancer (24), pancreatic cancer (25), prostate cancer (14), human glioblastoma (26), multiple myeloma (27), primary effusion leukemia (8), acute lymphoblastic leukemia (28), and myeloblastic leukemia (18).

Most cancer cells have higher levels of ROS that help in proliferation and cell growth. Typically, low doses of ROS are mitogenic and promote cell proliferation, while intermediate doses result in either temporary or permanent growth arrest, such as replicative senescence. Severe oxidative stress ultimately causes cell death via either apoptotic or necrotic mechanisms. Thus, a further increase of ROS in cancer cells using exogenous ROS-modulating agents is likely to cause elevation of ROS above the threshold level, ultimately leading to cell death (29). TQ is known to be redox active and to undergo one-electron and two-electron reduction processes by cellular reductases, leading to the corresponding semiquinone or hydroquinone,

## TQ induces apoptosis via ROS in malignant T cells

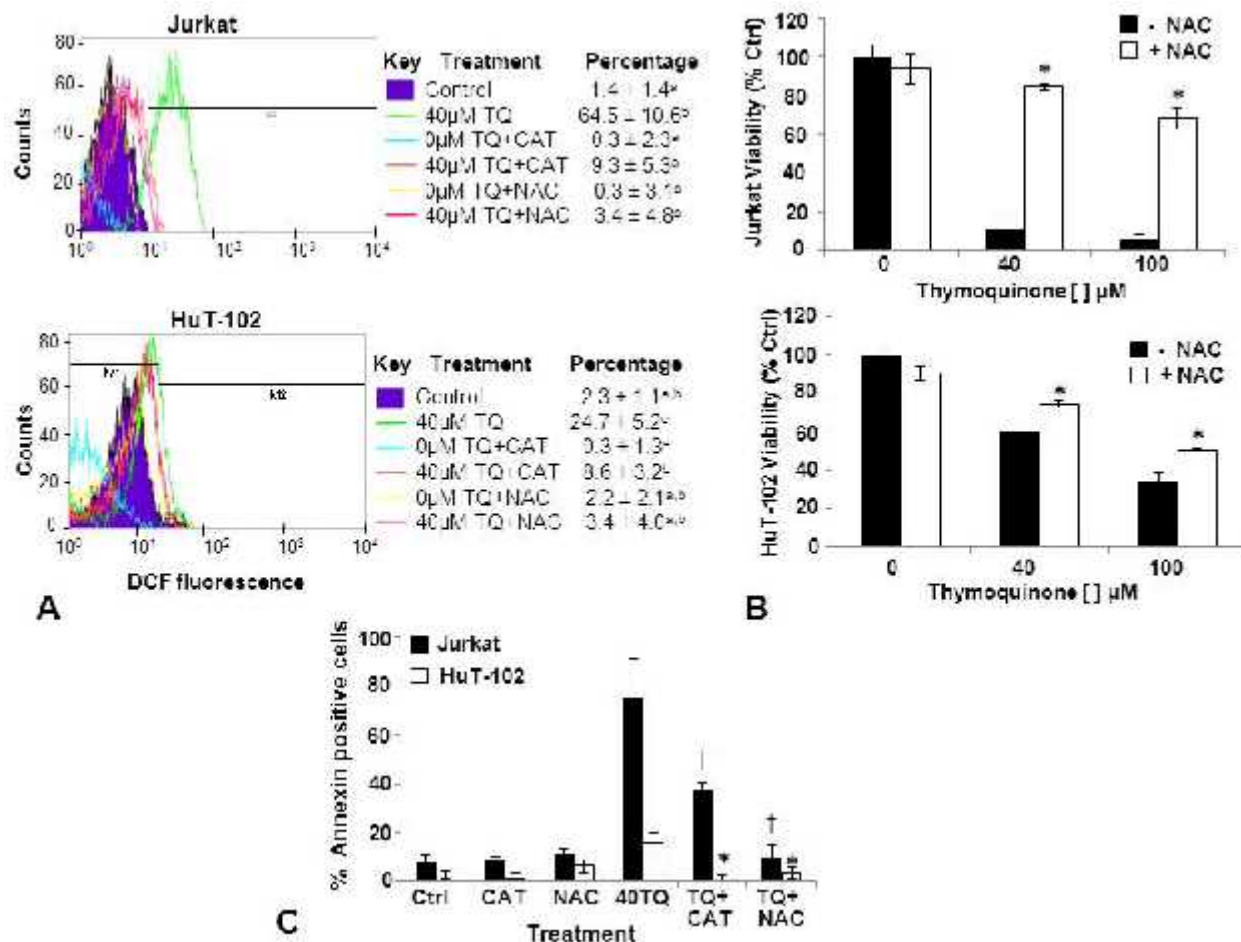


**Figure 6.** Pretreatment with NAC and CAT protects malignant T cells, especially Jurkat cells, against TQ-induced ROS generation and apoptosis. (A) Cells were pretreated with 5 mM NAC for 2 hours or with CAT (500 U/ml) for 5 min, after which 10 microM CM- H2DCFDA dye was added for 20 min. Cells were then treated with TQ for 1 hour, harvested and the amount of DCF fluorescence was analyzed immediately by flow cytometry. M2 indicates the increase in DCF fluorescence which indirectly measures ROS. Representative results are depicted which show 10,000 counts under each treatment condition. Each percentage is the mean  $\pm$  SD of three separate experiments. (B) Cells were treated with the antioxidant NAC (5 mM for 2 hours) followed by addition of TQ for 48 hours. Viability was determined by the MTT assay as described in “Materials and Methods”. Each value is the mean  $\pm$  SD of three separate experiments done in duplicates. \*significant difference ( $p < 0.05$ ) by one-tailed t-test between NAC pretreated and untreated samples. (C) Jurkat and HuT-102 were pretreated with 5 mM NAC for 2 hours or with CAT (500 U/ml) for 5 min, and then exposed to TQ for 48 hours. Cells were subsequently stained with fluorescein-conjugated annexin V and PI. Apoptotic cells were analyzed by flow cytometry. The graphs display the means  $\pm$  SD of two separate experiments each in duplicates. †\*significant difference ( $p < 0.05$ ) by one-tailed t-test between NAC or CAT pretreated and untreated HuT-102 (\*) or Jurkat (†).

respectively (30). These semiquinones ( $SQ^{\bullet-}$ ) react with molecular oxygen to produce superoxide ( $O_2^{\bullet-}$ ) and  $H_2O_2$ , the latter being the main source of generated ROS.

In this study, we present several lines of evidence indicating that ROS generation by TQ is responsible for its anticancer properties in malignant T-cells. First, high levels of intracellular ROS were generated in response to TQ as shown by the CM-H<sub>2</sub>DCFDA assay. Second, the greater depletion of intracellular GSH as well as the higher levels of ROS generated by TQ treatment of Jurkat cells in comparison to HuT-102 cells correlated with a larger apoptotic response in the former cell line. Third,

the strong antioxidant and GSH precursor, NAC, which restored ROS to basal levels, also significantly inhibited TQ's apoptotic effects, particularly in Jurkat cells. Fourth, exogenous CAT caused a lower inhibition of TQ-induced apoptosis than NAC; since NAC is a general ROS scavenger and glutathione precursor (31). Fifth, TQ treatment of normal PBMC did not generate ROS which may have a direct bearing on the lack of toxicity of TQ to these cells. The latter property makes TQ an interesting molecule as it enhances its selectivity to malignant T-cells. Reasons that could explain the minimal toxicity of TQ to normal lymphocytes is its well-documented dual oxidant properties depending on the physiological conditions and

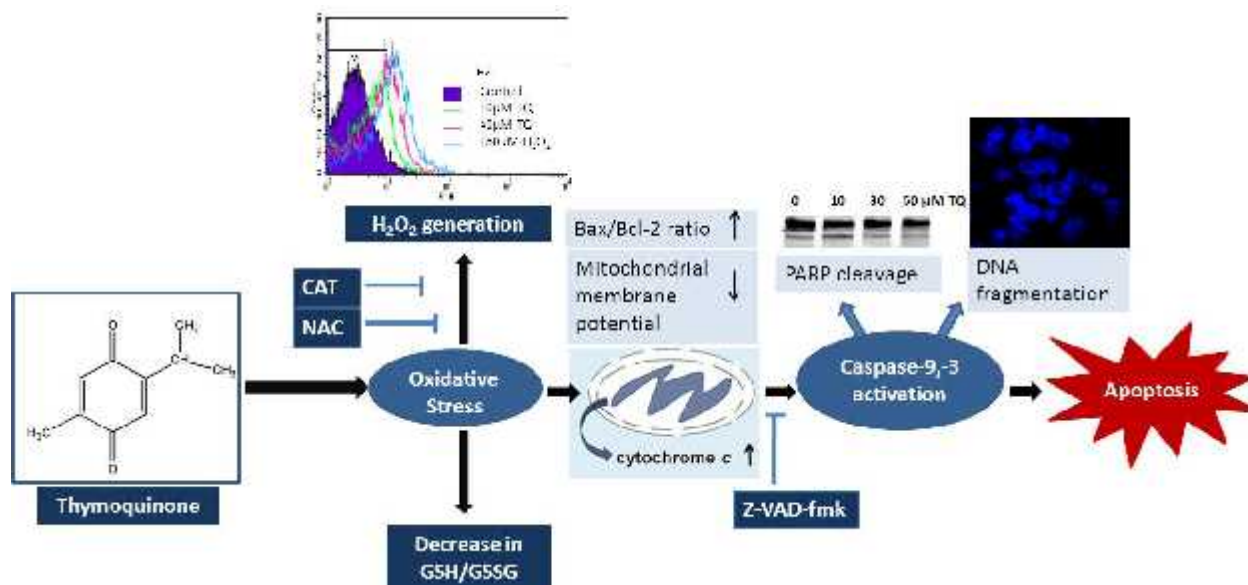


**Figure 7.** Schematic representation of the mechanism of TQ-induced apoptosis in malignant T-cells. TQ causes oxidative stress by increasing the generation of  $H_2O_2$  and depleting the antioxidant enzyme glutathione (GSH), thus leading to loss of mitochondrial membrane potential, the release of cytochrome *c*, activation of caspases 3 and 9, DNA fragmentation, and cleavage of the caspase-3 substrate poly(ADP-ribose) polymerase-1 apoptosis. The general caspase inhibitor z-VAD-fmk partially reversed TQ-induced apoptosis. N-acetyl cysteine (NAC) inhibited TQ-induced apoptosis more than catalase (CAT) (thicker arrow) because of its general ROS scavenging effects and ability to replenish cellular GSH that is depleted by TQ.

genetic profiles of cells. In several reports, TQ was shown to be an antioxidant by inhibiting iron-dependent microsomal lipid peroxidation, cardiotoxicity induced by doxorubicin in rats, and ifosfamide-induced damage in kidney (32). Therefore, although TQ has not been documented as an antioxidant in normal lymphocytes, it has shown antioxidant and prooxidant properties depending on the cell system (10). An increase in ROS generation by TQ in tumor cells is in accordance with other recent studies, including ours that have demonstrated ROS involvement in TQ-induced apoptosis (8,10,11,22).

Because the ROS produced by TQ may alter the cellular redox state through the oxidation of GSH, we analyzed the intracellular GSH content in malignant T-lymphocytes after treatment with TQ. GSH is a chief intracellular antioxidant responsible for maintaining redox balance. It is oxidized to form GSSG by the enzyme glutathione reductase and high concentrations of GSSG can oxidatively damage many critical enzymes (4). After 2 hours of 10 microM and 40 microM TQ, the GSH levels decreased to about 50% and 75% in Jurkat, while in HuT-102 a dose of 40 microM TQ was required to decrease GSH levels by 40% in comparison to control levels. A 10 fold higher concentration of TQ was required to deplete GSH content in HuT-102 to reach similar levels of Jurkat. This depletion of GSH could explain the greater sensitivity of Jurkat cells to TQ's apoptotic effects. Our results also corroborate the studies which show a decrease in the GSH/GSSG ratio with TQ treatment in prostate cancer cells (11). Alteration in the intracellular GSH content governs cell death pathways by inducing the mitochondrial permeability transition pore opening, leading to

mitochondrial membrane disruption and the release of pro-apoptotic factors. This is mainly due to the protection that GSH confers to the nearby thiol groups located in the mitochondrial permeability transition pore (33,34,35). Indeed, in accordance with GSH role in mitochondrial function, we observed a decrease in the mitochondrial membrane potential in TQ-treated malignant T cells, and the effect was more pronounced in Jurkat than HuT-102 cells. Since the mitochondrial function is regulated by Bcl-2 family proteins (36), we investigated the expression of the key proteins, Bax and Bcl-2, after TQ treatment. A significant increase in Bax expression and a decrease in Bcl-2 were observed after 24 hour of treatment with TQ. The increase in Bax/Bcl-2 ratio favors apoptosis induction, because Bcl-2 is known to inhibit apoptosis by negatively regulating the apoptotic activity of Bax. As a consequence of mitochondrial membrane damage, cytochrome *c* was released into the cytosol and was elevated by 8-fold in Jurkat cells (24 hours after 40 microM TQ) and only by 3-fold in HuT-102 (48 hours after 40 microM TQ). Furthermore, the caspase 9 activation in TQ-induced apoptosis supports the involvement of the intrinsic mitochondria-dependent apoptotic pathway.

Our data clearly indicate that the HTLV-1 negative cells are significantly more sensitive to TQ than HTLV-1 positive cells. The percentage of cells in the sub-G1 region was more than 7 fold higher in Jurkat than in HuT-102 cells treated with 40 microM TQ for 48 hours. The greater nuclear fragmentation and higher percentage of Annexin positive cells after TQ treatment in Jurkat cells also provides evidence for the higher cytotoxicity of TQ to this cell line compared to HuT-102 cells. The greater

resistance of HTLV-1 positive cells is in accordance with studies that show how Tax-induced constitutive activation of the NF- $\kappa$ B pathway may confer higher protection against anticancer drugs in these cells (37). Furthermore, HTLV-1 positive cells are known to over express levels of antiapoptotic factors such as Bcl-2, Bcl-xL and I-309 (38), survivin (39) and cellular proliferation markers such as Ki-67, and to over express MDR proteins involved in multidrug resistance (40).

Our work broadly describes the effects of TQ in four different leukemic cancer cell lines (Jurkat, CEM, HuT-102, and MT-2) and provides evidence for the involvement of ROS and the depletion of GSH levels in TQ-induced apoptosis in these cells. It is noteworthy to mention that several ROS modulating agents such as Elesclomol, Trisnex, and  $AS_2O_3$  are currently being used for the treatment of metastatic melanoma and acute promyelocytic leukemia, respectively. While both Elesclomol and Trisnex selectively kill cancer cells by increasing ROS generation,  $AS_2O_3$  kills cancer cells through the down regulation of endogenous antioxidant systems; namely glutathione peroxidase (GPx) and thioredoxine reductase (TrxR) (41,42). In contrast, TQ not only increases intracellular ROS but also decreases the levels of the antioxidant GSH ultimately playing a dual potentiating role in triggering oxidative stress-induced cell death making it very attractive for anticancer therapy.

## 6. ACKNOWLEDGEMENTS

This work was supported by Deutsche Forschungsgemeinschaft (SCHN477/7-3, SCHN477/7-4, SCHN477/12-2) and by the University Research Board of the AUB and the Lebanese National Council for Scientific Research.

## 7. REFERENCES

1. Jennifer Martindale, Nikki Holbrook: Cellular response to oxidative stress: Signaling for suicide and survival. *J Cell Physiol* 192, 1–15 (2002)
2. Nuran Ercal, Hande Gurer-Orhan, Nukhet Aykin-Burns: Toxic metals and oxidative stress part I: mechanisms involved in metal-induced oxidative damage. *Curr Top Med Chem* 1, 529–539 (2001)
3. Peter Stroz: Reactive oxygen species in tumor progression. *Front Biosci* 10, 1881–1896 (2005)
4. Christopher Jones, Able Lawrence, Peter Wardman, Marc Burkitt: Kinetics of superoxide scavenging by glutathione: an evaluation of its role in the removal of mitochondrial superoxide. *Biochem Soc Trans* 31, 1337–1339 (2003)
5. Dunyaporn Trachootham, Jerome Alexandre, Peng Huang: Targeting cancer cells by ROS-mediated mechanisms: a radical therapeutic approach? *Nat Rev Drug Discov* 8, 579–591 (2009)
6. Hala Gali-Muhtasib, Albert Roessner, Regine Schneider-Stock: Thymoquinone: a promising anti-cancer drug from

natural sources. *Int J Biochem Cell Biol* 38, 1249–1253 (2006)

7. Sanjeev Banerjee, Subhash Padhye, Asfar Azmi, Zhiwei Wang, Philip A. Philip, Omer Kucuk, Fazlul H. Sarkar, Ramzi M. Mohammad: Review on molecular and therapeutic potential of thymoquinone in cancer. *Nutr Cancer* 62, 938–946 (2010)
8. Azhar R. Hussain, Maqbool Ahmea, Saeeda Ahmed, Pulicat Manogaran, Leonidas C. Platanias, Syed N. Alvid, Khawla S. Al-Kuraya, Shahab Uddin: Thymoquinone suppresses growth and induces apoptosis via generation of reactive oxygen species in primary effusion lymphoma. *Free Radic Biol Med* 50, 978–987 (2011)
9. Katharina Effenberger-Neidnicht, Schobert Rainer: Combinatorial effects of thymoquinone on the anti-cancer activity of doxorubicin. *Cancer Chemother Pharmacol* 67, 867–874 (2011)
10. Nahed El-Najjar, Manal Chatila, Hiba Moukadem, Heikki Vuorela, Matthias Ocker, Muktheshwar Gandesiri, Regine Schneider-Stock, Hala Gali-Muhtasib: Reactive oxygen species mediate thymoquinone-induced apoptosis and activate ERK and JNK signaling. *Apoptosis* 15, 183–195 (2010)
11. Padma Sandeep Koka, Debasis Mondal, Michelle Schultz, Asim B Abdel-Mageed Krishna Agrawal: Studies on molecular mechanisms of growth inhibitory effects of thymoquinone against prostate cancer cells: role of reactive oxygen species. *Exp Biol Med (Maywood)* 235, 751–760 (2010)
12. Mahmoud Alhossin, Abdurazzag Abusnina, Mayada Achour, Tanveer Sharif, Christian Mulleb, Jean Peluso, Thierry Chataigneau, Claire Lugnier, Valérie B. Schini-Kerth, Christian Bronner, Guy Fuhrmann: Induction of apoptosis by thymoquinone in lymphoblastic leukemia Jurkat cells is mediated by a p73-dependent pathway which targets the epigenetic integrator UHRF1. *Biochem Pharmacol* 79, 1251–1260 (2010)
13. Sanjeev Banerjee, Ahmed Kaseb, Zhiwei Wang, Deujan Kong, Mussop Mohammad, Subhash Padhye, Fazlul H. Sarkar, Ramzi Mohammad: Antitumor activity of gemcitabine and oxaliplatin is augmented by thymoquinone in pancreatic cancer. *Cancer Res* 69, 5575–5583 (2009)
14. Ahmed Kaseb, Kannagi Chinnakannu, Di Chen, Arun Sivanandam, Sheela Tejwan, Mani Menon, Q. Ping Dou, G. Prem-Veer Reddy: Androgen receptor and E2F-1 targeted thymoquinone therapy for hormone refractory prostate cancer. *Cancer Res* 67, 7782–88 (2007)
15. Youmna Kfoury, Rihab Nasr, Olivier Hermine, Hugues de Thé, Ali Bazarbachi: Proapoptotic regimes for HTLV-I-transformed cells: targeting Tax and the

NF-kappaB pathway. *Cell Death Differ* 1, 871-877 (2005)

16. Bazarbachi Ali, Hermine Olivier: Treatment of adult T-cell leukaemia/lymphoma: current strategy and future perspectives. *Virus Res* 78, 79–92 (2001)

17. Wafica Itani, Sarah El-Banna, Saadia Hassan, Rolf Larsson, Ali Bazarbachi, Hala Gali-Muhtasib: Anti colon cancer components from Lebanese sage (*Salvia libanotica*) essential oil: Mechanistic basis. *Cancer Biol Ther* 7, 1765–1773 (2008)

18. Mohamed El-Mahdy, Qianzheng Zhu, Qi-En Wang, Gulzar Wani, Altaf Wani: Thymoquinone induces apoptosis through activation of caspase-8 and mitochondrial events in p53-null myeloblastic leukemia HL-60 cells. *Int J Cancer* 117, 409–417 (2005)

19. Martin Roepke, Antje Diestel, Khoulood Bajbouj, Diana Walluscheck, Peter Schonfeld, Albert Roessner, Regine Schneider-Stock, Hala Gali-Muhtasib: Lack of p53 augments thymoquinone-induced apoptosis and caspase activation in human osteosarcoma cells. *Cancer Biol Ther*, 6160–6169 (2007)

20. Hala Gali-Muhtasib, Doerthe Kuester, Christian Mawrin, Khoulood Bajbouj, Antje Diestel, Matthias Ocker, Caroline Hahold, Charlotte Foltzer-Jourdainne, Peter Schoenfeld, Brigitte Peters, Mona Diab-Assaf, Ulf Pommrich, Wafica Itani, Hans Lippert, Albert Roessner, Regine Schneider-Stock: Thymoquinone triggers inactivation of the stress response pathway sensor CHEK1 and contributes to apoptosis in colorectal cancer cells. *Cancer Res* 68, 5609–5618 (2008)

21. Mansouria Merad-Boudia, Annie Nicole, Dominique Santiard-Baron, Christophe Saillé, Irène Ceballos-Picot: Mitochondrial impairment as an early event in the process of apoptosis induced by glutathione depletion in neuronal cells: relevance to Parkinson's disease. *Biochem Pharmacol* 56, 645–655 (1998)

22. Hala Gali-Muhtasib, Matthias Ocker, Doerthe Kuester, Sabine Krueger, Zeina El-Hajj, Antje Diestel, Matthias Evert, Nahed El-Najjar, Brigitte Peters, Abdo Jurjus, Albert Roessner, Regine Schneider-Stock: Thymoquinone reduces mouse colon tumor cell invasion and inhibits tumor growth in murine colon cancer models. *J Cell Mol Med* 12, 330–342 (2008)

23. Hala Gali-Muhtasib, Wassim Abou Kheir, Lynn Kheir, Nadine Darwiche, Peter Crooks: Molecular pathway for thymoquinone-induced cell-cycle arrest and apoptosis in neoplastic keratinocytes. *Anticancer Drugs* 15, 389–99 (2004)

24. El-Shaimaa Arafa, Qianzheng Zhu, Zubair Shah, Gulzar Wani, Bassant Barakat, Ira Racoma, Mohamed El-Mahdy, Altaf Wani: Thymoquinone up-regulates PTEN expression and induces apoptosis in doxorubicin-resistant human breast cancer cells. *Mutat Res* 706, 28–35 (2011)

25. Maria Torres, Moorthy Ponnusamy, Subhankar Chakraborty, Lynette Smith, Srustidhar Das, Hwyda Arafat, Surinder Batra Torres: Effects of thymoquinone in the expression of mucin 4 in pancreatic cancer cells: implications for the development of novel cancer therapies. *Mol Cancer Ther*, 9, 1419–1431 (2010)

26. Kaouther Kolli-Bouhafs, Abdelaziz Boukhari, Abdurazzag Abusnina, Emilie Velot, Jean-Pierre Gies, Claire Lugnier, Philippe Rondé: Thymoquinone reduces migration and invasion of human glioblastoma cells associated with FAK, MMP-2 and MMP-9 down-regulation. *Invest New Drugs* (2011)

27. Gamal Badr, Eric Lefevre, Mohamed Mohany: Thymoquinone inhibits the CXCL12-induced chemotaxis of multiple myeloma cells and increases their susceptibility to Fas-mediated apoptosis. *PLoS One* 6, e23741 (2011)

28. Abdurazzag Abusnina, Mahmoud Alhosin, Thérèse Keravis, Christian Muller, Guy Fuhrmann, Christian Bronner, Claire Lugnier: Down-regulation of cyclic nucleotide phosphodiesterase PDE1A is the key event of p73 and UHRF1 deregulation in thymoquinone-induced acute lymphoblastic leukemia cell apoptosis. *Cell Signal* 23, 152–160 (2011)

29. Paul Schumacker: Reactive oxygen species in cancer cells: live by the sword, die by the sword. *Cancer Cell* 10, 175–176 (2006)

30. Anders Brunmark, Enrique Cadenas: Redox and addition chemistry of quinoid compounds and its biological implications. *Free Radic Biol Med* 7, 435–477 (1989)

31. Muhammad Zafarullah, Wei-qin Li, Judith Sylvester, Mansur Ahmad: Molecular mechanisms of N-acetylcysteine actions. *Cell Mol Life Sci* 60, 6–20 (2003)

32. Osama Badary, Ragia Taha, Ayman Gamal El-Din, Mohamed Abdel-Wahab: Thymoquinone is a potent superoxide anion scavenger. *Drug Chem Toxicol* 26, 87–98 (2003)

33. Silvia Coppola, Lina Ghibelli: GSH extrusion and the mitochondrial pathway of apoptotic signalling. *Biochem Soc Trans* 28, 56–61 (2000)

34. Mark Hampton, Bengt fadeel, Sten Orrenius: Redox regulation of the caspases during apoptosis. *Ann NY Acad Sci* 854, 328–335 (1998)

35. Guido Kroemer, Lorenzo Galluzzi, Catherine Brenner: Mitochondrial membrane permeabilization in cell death. *Physiol Rev* 87, 99–163 (2007)

36. Suzanne Cory, Jerry M. Adams: The Bcl-2 apoptotic switch in cancer development and therapy. *Oncogene* 26, 1324–1337 (2007)

37. Nadine Darwiche, Asma Hatoum, Ghaasan Dbaiibo, Humam Kadara, Rihab Nasr, Ghada Abou-Lteif, Bazzi R,

## TQ induces apoptosis via ROS in malignant T cells

Olivier Hermine, Hugues de Thé, Ali Bazarbachi: N-(4-hydroxyphenyl) retinamide induces growth arrest and apoptosis in HTLV-1-transformed cells. *Leukemia* 18, 607–615 (2004)

38. Andrea K. Kress, Ralph Grassmann, Bernhard Fleckenstein: Cell surface markers in HTLV-1 pathogenesis. *Viruses* 3, 1439–1459 (2011)

39. Hirochika Kawakami, Mariko Tomita, Takehiro Matsuda, Takao Ohta, Yuetsu Tanaka, Masahiro Fujii, Masahiko Hatano, Takeshi Tokuhisa, Naoki Mori: Transcriptional activation of survivin through the NF-kappaB pathway by human T-cell leukemia virus type I tax. *Int J Cancer* 115, 967–974 (2005)

40. Alan Lau, Simon Nightingale, Graham Taylor, Timothy Gant, Alan Cann: Enhanced MDR1 gene expression in human T-cell leukemia virus-I-infected patients offers new prospects for therapy. *Blood* 91, 2467–2474 (1998)

41. Jung-Yong Yeh, Lung-Chih Cheng, Bor-Rung Ou, DP Whanger, Larry Chang: Differential influences of various arsenic compounds on glutathione redox status and antioxidative enzymes in porcine endothelial cells. *Cell Mol Life Sci* 59, 1972–1982 (2002)

42. Jun Lu, Eng-Hui Chew, Arne Holmgren: Targeting thioredoxin reductase is a basis for cancer therapy by arsenic trioxide. *Proc Natl Acad Sci U S A* 104, 12288–12293 (2007)

**Abbreviations:** ROS: reactive oxygen species, GPX: glutathione peroxidase, GR: glutathione reductase, TRX: thioredoxin, SOD: superoxide dismutase, GSH :glutathione, GSSG: glutathione disulfide, TQ : Thymoquinone, ATL: Adult T cell leukemia/lymphoma, HTLV-1: T-cell lymphotropic virus type I, PBMC: peripheral blood mononuclear cells, NAC: N-acetyl cysteine, CAT: catalase, ELISA: enzyme-linked immunosorbent assay, BSO: buthionine sulfoximine, CM-H2DCFDA: 5-(and-6)-chloromethyl-2',7'-dichlorodihydrofluorescein diacetate, acetyl ester, DCF: 2'-7'-dichlorofluorescein

**Key Words:** T-cell leukemia, Thymoquinone, ROS, Apoptosis, Anticancer

**Send correspondence to:** Hala Gali-Muhtasib, Department of Biology, American University of Beirut, Beirut, Lebanon, Tel: 961350000 Ext:3894, Fax: 9611744461, E-mail: amro@aub.edu.lb